HHS Public Access

Author manuscript

J Hepatol. Author manuscript; available in PMC 2017 August 01.

Published in final edited form as:

J Hepatol. 2016 August ; 65(2): 334–343. doi:10.1016/j.jhep.2016.04.022.

Humanized mice efficiently engrafted with fetal hepatoblasts and syngeneic immune cells develop human monocytes and NK cells

Eva Billerbeck[1,†], **Michiel C. Mommersteeg**[1,†], **Amir Shlomai**[1], **Jing W. Xiao**[1], **Linda Andrus**[1], **Ankit Bhatta**[1], **Koen Vercauteren**[1], **Eleftherios Michailidis**[1], **Marcus Dorner**[1,2], **Anuradha Krishnan**[3], **Michael R. Charlton**[3], **Luis Chiriboga**[4], **Charles M. Rice**[1,*], and **Ype P. de Jong**[1,5,*]

[1]Laboratory of Virology and Infectious Disease, The Rockefeller University, New York, NY, USA

[3]Division of Gastroenterology and Hepatology, Mayo Clinic, Rochester, MN, USA

[4]Department of Pathology, New York University Medical Center, New York, NY, USA

[5]Division of Gastroenterology and Hepatology, Weill Cornell Medical College, New York, NY, USA

Abstract

Background & Aims—Human liver chimeric mice are useful models of human hepatitis virus infection, including hepatitis B and C virus infections. Independently, immunodeficient mice reconstituted with $CD34^+$ hematopoietic stem cells (HSC) derived from fetal liver reliably develop human T and B lymphocytes. Combining these systems has long been hampered by inefficient liver reconstitution of human fetal hepatoblasts. Our study aimed to enhance hepatoblast engraftment in order to create a mouse model with syngeneic human liver and immune cells.

Methods—The effects of human oncostatin-M administration on fetal hepatoblast engraftment into immunodeficient *fah−/−* mice was tested. Mice were then transplanted with syngeneic human hepatoblasts and HSC after which human leukocyte chimerism and functionality were analyzed by flow cytometry, and mice were challenged with HBV.

Results—Addition of human oncostatin-M enhanced human hepatoblast engraftment in immunodeficient *fah−/−* mice by 5–100 fold. In contrast to mice singly engrafted with HSC, which predominantly developed human T and B lymphocytes, mice co-transplanted with syngeneic hepatoblasts also contained physiological levels of human monocytes and natural killer cells. Upon infection with HBV, these mice displayed rapid and sustained viremia.

[*]Corresponding authors. Address: The Rockefeller University, Laboratory of Virology and Infectious Disease, 1230 York Avenue, Box 64, New York, NY 10065, USA. Tel.: +1 212 327 7009; fax: +1 212 327 7048. ricec@rockefeller.edu (C.M. Rice), ydj2001@med.cornell.edu (Y.P. de Jong).

[2]Present address: Section of Virology and Section of Hepatology, Imperial College London, London, UK

[†]These authors contributed equally as joint first authors.

Author's contributions

EB, MCM and YPJ designed the study, performed experiments and analyzed data; AS, JWX, LA, AB, KV, LM, MD and LC performed experiments; AK and MRC provided hepatocytes; CMR designed the study, analyzed data and edited the manuscript; EB and YPJ wrote the manuscript.

Supplementary data

Supplementary data associated with this article can be found, in the online version, at http://dx.doi.org/10.1016/j.jhep.2016.04.022.

Conclusions—Our study provides a new mouse model with improved human fetal hepatoblast engraftment and an expanded human immune cell repertoire. With further improvements, this model may become useful for studying human immunity against viral hepatitis.

Lay summary—Important human pathogens such as hepatitis B virus, hepatitis C virus and human immunodeficiency virus only infect human cells which complicates the development of mouse models for the study of these pathogens. One way to make mice permissive for human pathogens is the transplantation of human cells into immune-compromised mice. For instance, the transplantation of human liver cells will allow the infection of these so-called “liver chimeric mice” with hepatitis B virus and hepatitis C virus. The co-transplantation of human immune cells into liver chimeric mice will further allow the study of human immune responses to hepatitis B virus or hepatitis C virus. However, for immunological studies it will be crucial that the transplanted human liver and immune cells are derived from the same human donor. In our study we describe the efficient engraftment of human fetal liver cells and immune cells derived from the same donor into mice. We show that liver co-engraftment resulted in an expanded human immune cell repertoire, including monocytes and natural killer cells in the liver. We further demonstrate that these mice could be infected with hepatitis B virus, which lead to an expansion of natural killer cells. In conclusion we have developed a new mouse model that could be useful to study human immune responses to human liver pathogens.

Keywords

Xenotransplantation; Liver chimeric mice; Human immune cells; Hepatitis B virus

Introduction

Many human pathogens fail to infect small animals, limiting investigations to nonhuman primates or clinical observational studies. One strategy to study such pathogens *in vivo* is the engraftment of human tissues into mice. For example, human immune system (HIS) mice are widely used to study leukotropic pathogens like human immunodeficiency virus (HIV) and Epstein-Barr virus [1]. Separately, human liver chimeric mice have proven relevant models for investigations of HBV, hepatitis C virus (HCV) and malaria species [2–4].

Humanization of mice generally follows two principles: a human graft most efficiently develops when the mouse equivalent is impaired, and recipient mice are immunodeficient in order to prevent xenorejection. In the case of HIS mice, transplantation of human $CD34^+$ HSC into immunodeficient recipients, e.g. NOD *rag1*$^{-/-}$ *il2rγ*^{null} (NRG) mice, reliably results in the development of human T and B cells [1]. However, the development of human monocytes and natural killer (NK) cells is impaired in HIS mice, likely due to limited cross-reactivity of mouse and human hematopoietic cytokines, e.g. granulocyte-macrophage colony stimulating factor (GM-CSF), macrophage colony stimulating factor (M-CSF), interleukin(IL)-3 and IL-15 [1]. In the case of human liver chimeric animals, a form of mouse liver injury is combined with a murine immunodeficiency, typically lymphocyte deficiency [3]. After transplantation of adult or pediatric human hepatocytes in such models, the murine liver injury creates a niche and drives the proliferation of human hepatocytes in the mouse liver, and this can result in high human chimerism [5,6]. However, the required

murine immunodeficiency in these animals has precluded the study of cellular immune functions in human liver disease.

One solution to address this lack of cellular immunity in human liver chimeric mice is to combine transplantation of human hepatocytes with human HSC into the same recipients. This has recently been reported by transplanting adult human hepatocytes and mismatched HSC derived from fetal human liver tissue, which resulted in doubly engrafted animals [7,8]. However, to avoid allogeneic immune responses both grafts should be derived from the same human donor. Possible solutions include the generation of human hepatocytes and HSC from induced pluripotent stem cells (iPS cells). Human HSC can also be obtained from adults [9] but hepatocytes from these same individuals are rarely available. When fetal hepatoblasts are combined with syngeneic HSC the liver graft either was lost [7] or the engrafted hepatoblasts fail to expand to high levels [10,11]. Together, these findings suggest that allogeneic doubly reconstituted mice can be generated but that human fetal hepatoblasts insufficiently engraft human liver chimeric mice, which limits the generation of syngeneic doubly reconstituted mice.

Here we first set out to generate mice that were highly engrafted with fetal hepatoblasts, and then combined this model with HSC transplantation obtained from the same human donor. These doubly engrafted animals, which we term ‘HIS-Hep’ mice, display improved human monocyte and NK cell development compared to HIS mice and can support HBV infection.

Materials and methods

Generation of liver chimeric mice

Adult human hepatocytes were harvested from surgical resection specimens as described [12], shipped overnight and transduced with VSVg pseudotyped lentiviral particles encoding for firefly luciferase under the human albumin promoter (FLuc pp) [13] prior to transplantation. For human hepatoblast transplantation, human fetal livers were procured from Advanced Bioscience Resources, Inc. Fetal livers were cut with scissors into gel-like substance and digested with 0.05% collagenase (Roche) for 30 min at 37 °C. Cells were put over 100 μm cell strainer (BD Bioscience), washed with William’s E media and after resuspension allowed to sediment at 1 g for 1 h [13]. The cell pellet, designated the large cell fraction, was freshly transplanted or after culture for 3 days to 2 weeks as described [13]. Cultured cells were resuspended using Accumax (eBioscience). Mouse hepatocytes from adult mice or unfractionated embryonic day 14 fetal liver cells were obtained from Cre recombinase transgenic mice crossed to FLuc transgenic mice preceded by a floxed stop codon, both obtained from Jackson Labs. Using isoflurane anesthesia human or mouse cell suspensions were injected intrasplenically into *fah−/−rag2−/−il2rgnull* (FRG) [14,15] of either gender or female *fah−/−* NOD *rag1−/−il2rgnull* (FNRG) mice that were generated by 13 generation backcrossing of the *fah−/−* allele [16] to NOD *rag1−/−il2rgnull* (NRG) animals obtained from Jackson Labs. Human fetal hepatoblasts were transplanted at 2.5–5 × 10^5 cells per mouse, adult human hepatocytes at 2.5 × 10^6 cells per mouse, and mouse hepatocytes or fetal liver cells at 5 × 10^5 cells per mouse. Starting on the day of transplantation mice were cycled off the drug NTBC/nitisinone (Yecuris) as described by others [5,14].

Generation of doubly reconstituted HIS-Hep animals

For concurrent transplantation, adult (>6 week old) female FNRG mice were irradiated with 100 cGy 12–24 h prior to intrasplenic transplantation of 2.5–5 × 10^5 fresh fetal hepatoblasts and 1.5–2 × 10^5 freshly isolated syngeneic HSC. hOSM treatment was started one day after transplantation for 3–4 weeks while mice were cycled off NTBC. For sequential transplantation mice received fresh hepatoblasts and, once median human albumin levels reached >10 μg/ml levels, mice were irradiated and received cryopreserved syngeneic HSC. After HSC transplantation NTBC cycling continued. As negative controls NRG mice were doubly transplanted or female FNRG mice were singly transplanted with HSC and cycled off the drug NTBC in parallel to doubly transplanted FNRG mice.

Ethics statement

All human materials were obtained after written informed consent was obtained from patients. The use of these materials was reviewed and approved by the Institutional Review Boards of the Rockefeller University, Weill Cornell Medical College and Mayo Clinics. All procedures involving mice were in accord with the National Institutes of Health (NIH) Guide for the Care and Use of Laboratory Animals and approved by the Rockefeller University Institutional Animal Care and Use Committees (protocol 12536).

All other methods are described in the Supplementary materials and methods section.

Results

Hepatoblasts inefficiently reconstitute mouse livers

Since the large cell fraction of human fetal liver contains hepatoblasts, we set out to create human liver chimeric mice starting with this fraction, from here on referred to as hepatoblasts. After transplantation of fresh or *in vitro* cultured [13] hepatoblasts into fumaryl acetoacetate hydrolase deficient (*fah*$^{-/-}$)*rag2*$^{-/-}$ *il2rγ*^{null} (FRG) mice [5,14] no human albumin (hAlb) (Supplementary Fig. 1A) or human transferrin (hTF) could consistently be detected in mouse serum. In order to distinguish whether this was due to a failure to engraft or to proliferate after transplantation, we transduced fresh hepatoblasts with firefly luciferase (FLuc) lentiviral vectors. In some recipients, a luminescent signal could be detected (Supplementary Fig. 1B) for up to 4 months after transplantation. However, and in contrast to adult hepatocytes, the luminescent signal did not consistently increase over this time period (Supplementary Fig. 1C). Because this could be due to an inherent inability of hepatoblasts to proliferate in such models [7,17] or because certain factors cross-react poorly between mouse and human, we next attempted to reconstitute FRG livers with murine hepatoblasts expressing FLuc. Adult mouse hepatocytes engrafted faster and at higher frequency than embryonic day 14 mouse liver cells, but several fetal cell recipients showed luminescence that started rising after approximately 2 months (Supplementary Fig. 1D). This suggested that mouse fetal liver cells had the ability to reconstitute FRG livers, albeit with lower efficiency than adult mouse hepatocytes. We therefore hypothesized that one or more factors required for human hepatoblast engraftment were not provided by the murine recipient and this explained the lack of efficient proliferation of human hepatoblasts.

Human oncostatin-M enhances human hepatoblast engraftment

Oncostatin-M (OSM) is expressed late in embryonic liver development [18] and required for *in vitro* differentiation of stem cells into hepatocyte-like cells [19,20]. We hypothesized that mouse OSM (mOSM) might fail to activate human hepatoblasts, impairing or limiting their proliferation after transplant. We therefore tested the induction of STAT3 phosphorylation in human hepatoma cell lines by mOSM. As opposed to human OSM (hOSM), dose dependent STAT3 phosphorylation was not observed with mOSM in HepG2 (Fig. 1A) or Huh7 (data not shown) hepatoma cells. This lack of mouse to human cross-reactivity was confirmed on primary human fetal liver cultures (HFLC) [13], whereas mOSM was able to activate murine H2-35 hepatoma cells (Fig. 1A). We then tested the ability of hOSM to enhance hepatoblast engraftment into immunodeficient *fah*$^{-/-}$ mice. We had previously observed that *fah*$^{-/-}$ mice crossed to NRG animals, designated FNRG mice, were superior recipients for adult human hepatocytes [21] than previously described FRG mice [5,14]. We therefore transplanted FNRG mice with human hepatoblasts and treated the mice with intraperitoneal injections of hOSM for 3 weeks, which resulted in a modest enhancement of hAlb and hTF serum levels early after transplantation (Fig. 1B). Serial measurements of hAlb serum levels showed that this early enhancement persisted over time, and that control-treated animals only displayed rising hAlb levels starting more than 2 months after transplantation (Fig. 1C). Because FRG recipients are more robust than FNRG mice, we found that hydrodynamic delivery (HDD) of a hOSM expression plasmid into FRG mice was associated with even more rapidly increasing and higher serum hAlb levels (45 fold over intraperitoneal hOSM injections, 182 fold over green fluorescent protein (GFP) HDD, day 52 post-transplant) than controls (Fig. 1D) ($p = 0.02$ for combined HDD experiments). Survival 3 months after plasmid HDD, fetal hepatoblast transplantation and NTBC cycling were 25–43% for mice that received GFP and 0–17% for those that received hOSM. The effect of hOSM substitution on hAlb serum levels was, to a variable degree, observed in 7 out of 7 human donors and was dependent on the *fah* −/− liver injury background (Fig. 1E). Histological analysis of livers from human hepatoblast transplanted FRG mice with high serum hAlb showed multiple islands of human hepatocytes, whereas animals with intermediate serum hAlb levels contained few islands (Fig. 1F), similar to what is typically observed after transplantation of adult human hepatocytes (data not shown). Human hepatocytes, which were identified by fumaryl acetoacetate hydrolase (FAH) and human-specific nuclear mitotic apparatus staining (Supplementary Fig. 2A), morphologically resembled human cells in FRG mice transplanted with adult human hepatocytes [21] and there was a correlation between serum albumin levels and the number of FAH+ islands in fetal hepatoblast transplanted mice (Supplementary Fig. 2B). In addition to human hepatocytes human endothelial cells could be detected in some mice engrafted with fetal hepatoblasts (Fig. 1G). These experiments indicate that hOSM administration enhanced otherwise inefficient human hepatoblast engraftment.

Hepatoblast engrafted mice can support hepatitis virus infection

We next tested the ability of these grafts to support HCV and HBV infections, both of which cannot infect mouse hepatocytes. Starting with mice that contained high serum hAlb levels (3.3–9.1 mg/ml), previously shown to be required to detect HCV viremia [5,22], animals were challenged with HCV. In one out of two, donors' viremia was detectable for months

whereas the second donor showed intermittently detectable viremia (Fig. 2A). Next, mice with more variable hAlb serum levels (404–9019 μg/ml) were challenged with plasma derived from an eAg negative HBV infected patient. HBV viremia (Fig. 2B) and HBV surface antigen (HBsAg) became detectable in all challenged mice (Fig. 2C), whereas no eAg could be detected (data not shown). Clusters of cAg+ hepatocytes could be observed in the livers of HBV viremic mice (Supplementary Fig. 2C). Three HBV viremic mice were treated with the nucleoside analogue entecavir. This suppressed HBV viremia but minimally affected the HBsAg levels (Fig. 2D), similar to previously published data on liver chimeric models [23,24] and in line with clinical observations. These results show that FRG mice that are highly engrafted with human hepatoblasts displayed similar characteristics for HBV and HCV infection as human liver chimeric models engrafted with adult human hepatocytes [5,22,23].

Dual reconstitution with syngeneic human liver and immune cells

Because NRG mice are commonly used for human immune cell reconstitution and the generation of HIS mice [1,25] we hypothesized that FNRG mice might provide a suitable background for generating mice dually reconstituted with human liver and immune cells derived from the same fetal liver, or HIS-Hep mice.

First, we compared the efficiency of human hematopoietic cell reconstitution in NRG *vs.* FNRG mice. When we transplanted same donor derived $CD34^+$ HSC into newborn NRG, $FAH^{+/-}$ NRG and $FAH^{-/-}$ NRG littermates from the F_{13} backcross of the FRG to the NOD background we found comparable human leukocyte subset reconstitution in the blood at week 12 post transplantation (Fig. 3A) indicating that F_{13} FNRG mice support efficient human immune system reconstitution and all subsequent studies were done exclusively in FNRG mice.

Next, we tested dual reconstitution of adult FNRG mice by either concurrent or sequential transplantation of syngeneic human fetal hepatoblasts and $CD34^+$ HSC as illustrated in Fig. 3B. Using this protocol we generated 7 independent cohorts of HIS-Hep mice, each cohort using a different human donor. The data shown in this study is combined data from mice that were either sequentially or concurrently transplanted (Fig. 3B) and received either hOSM or control medium. Characteristics of all HIS-Hep mice are listed in Supplementary Table 1.

Human leukocyte chimerism in blood, spleen and liver of HIS-Hep mice ranged from 10–90% (Fig. 3C–D) at week 12-post transplantation. They also exhibited substantial T and B cell (Fig. 3C) and dendritic cell (data not shown) reconstitution. At week 12-post transplantation, T cells comprised about 70% $CD4^+$ and 30% $CD8^+$ T cells in liver and blood (Fig. 3E). Of note, this ratio is invers in the human liver indicating a possibly impaired homing or recruitment of $CD8^+$ T cells to the liver in humanized mice. T cells from HIS-Hep mice produced IFN-γ, TNF-α, perforin and granzyme B upon isolation and *in vitro* stimulation with PMA/Ionomycin (Fig. 3F).

Improved development of human monocytes and NK cells in HIS-Hep mice

Previously reported HIS mouse models exhibit impaired development of human monocytes and NK cells [1]. In HIS-Hep mice, however, we observed robust development of human

$CD14^+$ monocytes and $CD56^+$ NK cells (Fig. 4A, C) at week 12-post human HSC transplantation. This was not HSC donor dependent as similar results were obtained for all 7 cohorts (Fig. 4A). $CD3^+$ $CD56^+$ NK T cell development was not improved in HIS-Hep mice (Fig. 4C).

When we generated HIS-NRG mice and HIS-Hep FNRG mice from the same human HSC donor we found a higher frequency of monocytes and NK cells in blood and liver of HIS-Hep mice (Fig. 4B, C). In addition, these mice showed higher peripheral monocyte and NK cell frequencies as compared to HIS-FNRG mice generated using the same human HSC donor and the same NTBC cycling protocol to induce murine liver damage (Fig. 4D). These results suggest that induction of murine liver injury itself is not sufficient to induce an improved monocyte and NK cell development. Further, this phenotype was independent of hOSM administration. Indeed, there was no correlation between frequencies of monocytes and NK cells and hOSM treatment in HIS-Hep from the same cohort (data not shown). To further confirm that hOSM does not directly induces the development of these cell subsets we transplanted FNRG mice with $CD34^+$ HSC only (HIS-FNRG) and treated them with hOSM. We detected comparable low frequencies of human monocytes and NK cells in blood and liver of hOSM treated HIS-FNRG mice as compared to untreated controls (Supplementary Fig. 3A and B).

In summary these results clearly indicate improved human monocyte and NK cell reconstitution is specific for HIS-Hep mice.

Monocytes and NK cells of HIS-Hep mice resemble human counterparts in phenotype, function and tissue distribution

NK cells are about 3-fold enriched in the human liver compared to the peripheral blood [26,27]. In line with this, we observed significant intrahepatic enrichment of NK cells in HIS-Hep mice (Fig. 4A). Human NK cells can be divided into two subsets: $CD56^{bright}CD16^-$ and $CD56^{dim}CD16^+$ cells [28]. About 90% of peripheral NK cells are $CD56^{dim}CD16^+$ while intrahepatic NK cells are enriched in the $CD56^{bright}$ $CD16^-$ subset [26]. We detected both NK cell subsets in HIS-Hep mice with a distribution similar to humans (Fig. 5A, B). NK cells exhibited high expression levels of the activating receptors NKp46 and NKp30, variable expression levels of NKG2A and NKG2C and low expression of Trail (Fig. 5C). Similar expression patterns of these receptors have been described for NK cells in humans [29].

When stimulated with PMA/Ionomycin HIS-Hep human NK cells produced IFN-γ, granzyme B and perforin, which was most pronounced in the liver (Fig. 5D). We further examined functionality of these cells by co-culturing intrahepatic NK cells with the human NK cell target cell line K562. NK cells produced IFN-γ and/or showed degranulation activity as indicated by CD107a expression (Fig. 5E, F).

Human monocytes can be divided into $CD14^+CD16^-$, $CD14^+$-$CD16^+$ and $CD14^-CD16^+$ subsets [30]. We detected all 3 subsets in blood and liver (Fig. 4C and Fig. 5G) of HIS-Hep animals. There was also a significant accumulation of monocytes in the liver as compared to the blood (Fig. 4A), which was most pronounced for the $CD14^+CD16^+$ subset (Fig. 5G, H).

Immunohistochemistry for the monocyte/Kupffer cell marker human CD68 confirmed that these cells morphologically resembled Kupffer cells in the chimeric liver (Fig. 5I) that could also be seen on H&E staining (Supplementary Fig. 4D). Similar to monocytes in humans and other humanized mouse models [31], monocytes in HIS-Hep mice showed high surface expression of CD33, CD11b, CD62L, CD115 and CXCR1 (Supplementary Fig. 4A–B) and produce IL-6 upon stimulation with lipopolysaccharide (LPS) or R848 (Supplementary Fig. 4C).

Taken together, these data demonstrate that HIS-Hep mice provide an environment that can promote development of functional human NK cells and monocytes.

Increased frequency of human NK cells during early HBV infection in HIS-Hep mice

To determine the potential utility of HIS-Hep mice for the study of human immune responses to a hepatotropic pathogen we next tested their susceptibility to HBV infection. HIS-Hep mice displayed rapid and sustained viremia when infected with 9.8×10^8 (cohort 1), 2.6×10^7 (cohort 3) and 3.5×10^6 (cohort 5) particles of mouse passaged HBV originally derived from an eAg- patient (Fig. 6A). Mice of cohort 3 and 5 were sacrificed for a cellular analysis at day 20-post infection and mice of cohort 1 at day 40-post infection.

Interestingly, during early HBV infection we detected a specific increase in the frequency of peripheral NK cells, but not T cells or monocytes, in HBV infected HIS-Hep mice as compared to controls (Fig. 6B). A similar trend was detectable in the liver, but not the spleen (Fig. 6C). These results are in line with reports of increased peripheral NK cell levels in early acute HBV in humans [32,33]. Peripheral but not intrahepatic NK cells of HBV infected mice also showed a higher expression of NKp30 as compared to controls (Fig. 6D) indicating NK cell activation in these mice.

In summary, these results indicate that HIS-Hep mice can be infected with HBV and show human NK cell activation during early HBV infection.

Discussion

Human hepatocytes obtained from pediatric or young adult donors generally engraft more efficiently in chimeric mouse models than those obtained from older donors [22]. Fetal hepatoblasts might be expected to have superior engraftment potential but several reports [7,17] and anecdotal evidence suggested that these cells engraft poorly. Our findings indicate that they do survive in the murine liver for months but inefficiently proliferate in response to the signals provided by the *fah*−/− liver injury model. Treatment with hOSM significantly enhanced fetal hepatoblast engraftment as compared to controls across several different human donors. Whereas HDD of a hOSM expression plasmid resulted in more efficient engraftment than daily i.p. injections, increased mortality was observed at higher plasmid doses. This was not seen after HDD of high doses of GFP expression plasmid or after i.p. injections. Furthermore, a second HDD of hOSM 3 months after transplantation did not further enhance hAlb levels. This suggests that hOSM dosing should be further optimized early after transplantation. Other delivery methods may result in superior hepatoblast engraftment while preventing mortality caused by excess hOSM. Mechanisms by which

hOSM might improve fetal hepatoblast engraftment and expansion remain unclear and may involve providing a signal for the maturation of hepatoblasts into hepatocytes that subsequently respond to the murine liver injury, a direct proliferative effect of hOSM on hepatoblasts, or indirect effects by causing changes in the mouse liver than subsequently lead to human hepatoblast differentiation and proliferation. It will also be important to determine which cells from the fetal large cell fraction engraft in FRG livers. We speculate that fetal hepatoblasts engraft but have not excluded the possibility that a subset of cells that have further matured toward hepatocytes repopulate the liver, nor what other cell types may be required. For example it is possible that human liver endothelial cells, which we identified in some mice, or other non-parenchymal cells present in the large cell fraction are required for efficient hepatoblast engraftment.

Since hOSM administration led to efficient engraftment of human hepatoblasts we were able to develop a new syngeneic HIS-Hep mouse model. We generated HIS-Hep mice by sequential or concurrent transplantation. While both protocol resulted in efficient hepatoblast and immune cell reconstitution our study cannot conclude which protocol is superior due to the limited number of cohorts generated.

HIS-Hep mice displayed a striking cellular immune phenotype. Conventional HIS mice and previously reported doubly reconstituted mice predominantly contain human T and B lymphocytes [1,10,11] while the development of monocytes and NK cells is impaired. In contrast, HIS-Hep mice consistently had physiological numbers of human monocytes and NK cells. As was recently reported using a human IL-3, M-CSF, GM-CSF knock-in approach, Rongvaux and colleagues were able to reconstitute HIS mice with human monocytes and NK cells to frequencies similar to those observed in our HIS-Hep mice [31]. Mechanisms that contribute to the improved monocyte and NK cell reconstitution in HIS-Hep mice will be determined in future studies.

Similar to Rongvaux *et al.* [31] we have observed a higher mortality (on average 47 ± 28%, range 13–83%) than typically observed in singly HSC or hepatoblast transplanted animals. This will need to be resolved in order to create larger cohorts of mice. In addition, similar to other HIS mouse models [1], HIS-Hep mice do not have a fully functional human immune system. To achieve this additional improvements will be necessary. One problem is the priming and function of T cells due to a lack of HLA expression in mice. Hepatoblasts engrafted express HLA, which likely enables human T cell recognition in the liver. Future improvements will include the generation of HIS-Hep mice in HLAtransgenic strains to also ensure HLA selection in the thymus. Future studies will also address if HLA expression on hepatoblasts can improve NK cell function through killer immunoglobulin-like receptor interactions with HLA molecules.

An increasing body of literature also suggests a role for NK cells during HBV infection [34]. Thus, an application of the HIS-Hep mouse model is the study of human NK cells and monocytes in human hepatotropic infections such as HBV, which have been notoriously plagued by limited access to human liver tissue. In our analysis of early acute HBV infection we did not observe an effect of immune cells on HBV infection, e.g., there was no decrease in viremia associated the presence of NK cells. Future studies need to address the effects of

immune cells on HBV viremia and other virological aspects in HIS-Hep mice, especially during longer infection periods.

In conclusion we have created a new humanized mouse model with efficient syngeneic human leukocytes and liver engraftment. We expect that this model will serve as a useful basis for further improvement strategies in order to develop a functional model for the study of human viral hepatitis.

Supplementary Material

Refer to Web version on PubMed Central for supplementary material.

Acknowledgments

Financial support

This work was funded by the National Institutes of Health through the NIH Roadmap for Medical Research, Grant 1 R01 DK085713 and the Starr Foundation (to CMR). This work was also supported in part by grants from National Institute of Diabetes and Digestive and Kidney Diseases, K08DK090576 (to YPJ) and the Center for Advanced Digestive Care at Weill Cornell Medical Center through the Helmsley Trust (to YPJ). The IHC core laboratory at NYU Medical Center is funded in part by the NYU Cancer Institute. The NYU Cancer Center is supported in part by grant 5P30CA016087-32 from the National Cancer Institute. The content is solely the responsibility of the authors and does not necessarily represent the official views of the National Institute of Diabetes and Digestive and Kidney Diseases or the National Institutes of Health.

We thank Dr Jose Jessurun for analyzing the histology, Dr Mayla Hsu for editing the manuscript, Dr Wayne Yokoyama for critically reviewing the manuscript, Rachel Labitt for mouse husbandry and Dr Alexander Ploss for help with the generation of mice.

Abbreviations

NK cell	natural killer cell
HBV	hepatitis B virus
HSC	hematopoietic stem cell
HIS	human immune system
HIS-Hep mice	mice with human immune system and liver xenograft
HCV	hepatitis C virus
fah	fumaryl acetoacetate hydrolase
hAlb	human serum albumin
NRG	NOD *rag1*$^{-/-}$ *il2rγnull* mouse
FRG	*fah*−/−*rag2*−/−*il2rgnull* mouse
FNRG	*fah*−/− NOD *rag1*−/−*il2rgnull* mouse
NTBC	2-(2-nitro-4-fluoromethylbenzoyl)-1,3-cyclohexanedione
OSM	oncostatin-M

References

Author names in bold designate shared co-first authorship

1. Shultz LD, Brehm MA, Garcia-Martinez JV, Greiner DL. Humanized mice for immune system investigation: progress, promise and challenges. Nat Rev Immunol. 2012; 12:786–798. [PubMed: 23059428]
2. Dandri M, Lutgehetmann M, Petersen J. Experimental models and therapeutic approaches for HBV. Semin Immunopathol. 2013; 35:7–21. [PubMed: 22898798]
3. Grompe M, Strom S. Mice with human livers. Gastroenterology. 2013; 145:1209–1214. [PubMed: 24042096]
4. Billerbeck E, de Jong Y, Dorner M, de la Fuente C, Ploss A. Animal models for hepatitis C. Curr Top Microbiol Immunol. 2013; 369:49–86. [PubMed: 23463197]
5. Bissig KD, Wieland SF, Tran P, Isogawa M, Le TT, Chisari FV, et al. Human liver chimeric mice provide a model for hepatitis B and C virus infection and treatment. J Clin Invest. 2010; 120:924–930. [PubMed: 20179355]
6. Tateno C, Yoshizane Y, Saito N, Kataoka M, Utoh R, Yamasaki C, et al. Near completely humanized liver in mice shows human-type metabolic responses to drugs. Am J Pathol. 2004; 165:901–912. [PubMed: 15331414]
7. Gutti TL, Knibbe JS, Makarov E, Zhang J, Yannam GR, Gorantla S, et al. Human hepatocytes and hematolymphoid dual reconstitution in treosulfan-conditioned uPA-NOG mice. Am J Pathol. 2014; 184:101–109. [PubMed: 24200850]
8. Wilson EM, Bial J, Bial G, Jensen B, Greiner DL, Brehm MA, et al. Extensive double humanization of both liver and hematopoiesis in FRGN mice. Stem Cell Res. 2014; 13:404–412. [PubMed: 25310256]
9. Smith TJ, Khatcheressian J, Lyman GH, Ozer H, Armitage JO, Balducci L, et al. 2006 update of recommendations for the use of white blood cell growth factors: an evidence-based clinical practice guideline. J Clin Oncol. 2006; 24:3187–3205. [PubMed: 16682719]
10. Washburn ML, Bility MT, Zhang L, Kovalev GI, Buntzman A, Frelinger JA, et al. A humanized mouse model to study hepatitis C virus infection, immune response, and liver disease. Gastroenterology. 2011; 140:1334–1344. [PubMed: 21237170]
11. Bility MT, Cheng L, Zhang Z, Luan Y, Li F, Chi L, et al. Hepatitis B virus infection and immunopathogenesis in a humanized mouse model: induction of human-specific liver fibrosis and M2-like macrophages. PLoS Pathog. 2014; 10:e1004032. [PubMed: 24651854]
12. Krishnan A, Viker K, Rietema H, Telgenkamp M, Knudsen B, Charlton M. Prolonged engraftment of human hepatocytes in mice transgenic for the deleted form of human hepatocyte growth factor. Hepatol Res. 2007; 37:854–862. [PubMed: 17573952]
13. Andrus L, Marukian S, Jones CT, Catanese MT, Sheahan TP, Schoggins JW, et al. Expression of paramyxovirus V proteins promotes replication and spread of hepatitis C virus in cultures of primary human fetal liver cells. Hepatology. 2011; 54:1901–1912. [PubMed: 22144107]
14. Azuma H, Paulk N, Ranade A, Dorrell C, Al-Dhalimy M, Ellis E, et al. Robust expansion of human hepatocytes in Fah−/−/Rag2−/−/Il2rg−/− mice. Nat Biotechnol. 2007; 25:903–910. [PubMed: 17664939]
15. Bissig KD, Le TT, Woods NB, Verma IM. Repopulation of adult and neonatal mice with human hepatocytes: a chimeric animal model. Proc Natl Acad Sci U S A. 2007; 104:20507–20511. [PubMed: 18077355]
16. Grompe M, Lindstedt S, al-Dhalimy M, Kennaway NG, Papaconstantinou J, Torres-Ramos CA, et al. Pharmacological correction of neonatal lethal hepatic dysfunction in a murine model of hereditary tyrosinaemia type I. Nat Genet. 1995; 10:453–460. [PubMed: 7545495]
17. Haridass D, Yuan Q, Becker PD, Cantz T, Iken M, Rothe M, et al. Repopulation efficiencies of adult hepatocytes, fetal liver progenitor cells, and embryonic stem cell-derived hepatic cells in albumin-promoter-enhancer urokinase-type plasminogen activator mice. Am J Pathol. 2009; 175:1483–1492. [PubMed: 19717639]

18. Kamiya A, Gonzalez FJ, Nakauchi H. Identification and differentiation of hepatic stem cells during liver development. Front Biosci. 2006; 11:1302–1310. [PubMed: 16368517]
19. Schwartz RE, Trehan K, Andrus L, Sheahan TP, Ploss A, Duncan SA, et al. Modeling hepatitis C virus infection using human induced pluripotent stem cells. Proc Natl Acad Sci U S A. 2012; 109:2544–2548. [PubMed: 22308485]
20. Si-Tayeb K, Lemaigre FP, Duncan SA. Organogenesis and development of the liver. Dev Cell. 2010; 18:175–189. [PubMed: 20159590]
21. de Jong YP, Dorner M, Mommersteeg MC, Xiao JW, Balazs AB, Robbins JB, et al. Broadly neutralizing antibodies abrogate established hepatitis C virus infection. Sci Transl Med. 2014; 6:254ra129.
22. Vanwolleghem T, Libbrecht L, Hansen BE, Desombere I, Roskams T, Meuleman P, et al. Factors determining successful engraftment of hepatocytes and susceptibility to hepatitis B and C virus infection in uPA-SCID mice. J Hepatol. 2010; 53:468–476. [PubMed: 20591528]
23. Allweiss L, Volz T, Lutgehetmann M, Giersch K, Bornscheuer T, Lohse AW, et al. Immune cell responses are not required to induce substantial hepatitis B virus antigen decline during pegylated interferon-alpha administration. J Hepatol. 2014; 60:500–507. [PubMed: 24398036]
24. Kosaka K, Hiraga N, Imamura M, Yoshimi S, Murakami E, Nakahara T, et al. A novel TK-NOG based humanized mouse model for the study of HBV and HCV infections. Biochem Biophys Res Commun. 2013; 441:230–235. [PubMed: 24140055]
25. Brehm MA, Cuthbert A, Yang C, Miller DM, DiIorio P, Laning J, et al. Parameters for establishing humanized mouse models to study human immunity: analysis of human hematopoietic stem cell engraftment in three immunodeficient strains of mice bearing the IL2rgamma(null) mutation. Clin Immunol. 2010; 135:84–98. [PubMed: 20096637]
26. Burt BM, Plitas G, Zhao Z, Bamboat ZM, Nguyen HM, Dupont B, et al. The lytic potential of human liver NK cells is restricted by their limited expression of inhibitory killer Ig-like receptors. J Immunol. 2009; 183:1789–1796. [PubMed: 19587011]
27. Crispe IN. The liver as a lymphoid organ. Annu Rev Immunol. 2009; 27:147–163. [PubMed: 19302037]
28. Cooper MA, Fehniger TA, Caligiuri MA. The biology of human natural killer-cell subsets. Trends Immunol. 2001; 22:633–640. [PubMed: 11698225]
29. Jost S, Altfeld M. Control of human viral infections by natural killer cells. Annu Rev Immunol. 2013; 31:163–194. [PubMed: 23298212]
30. Auffray C, Sieweke MH, Geissmann F. Blood monocytes: development, heterogeneity, and relationship with dendritic cells. Annu Rev Immunol. 2009; 27:669–692. [PubMed: 19132917]
31. Rongvaux A, Willinger T, Martinek J, Strowig T, Gearty SV, Teichmann LL, et al. Development and function of human innate immune cells in a humanized mouse model. Nat Biotechnol. 2014; 32:364–372. [PubMed: 24633240]
32. Webster GJ, Reignat S, Maini MK, Whalley SA, Ogg GS, King A, et al. Incubation phase of acute hepatitis B in man: dynamic of cellular immune mechanisms. Hepatology. 2000; 32:1117–1124. [PubMed: 11050064]
33. Fisicaro P, Valdatta C, Boni C, Massari M, Mori C, Zerbini A, et al. Early kinetics of innate and adaptive immune responses during hepatitis B virus infection. Gut. 2009; 58:974–982. [PubMed: 19201769]
34. Rehermann B. Pathogenesis of chronic viral hepatitis: differential roles of T cells and NK cells. Nat Med. 2013; 19:859–868. [PubMed: 23836236]

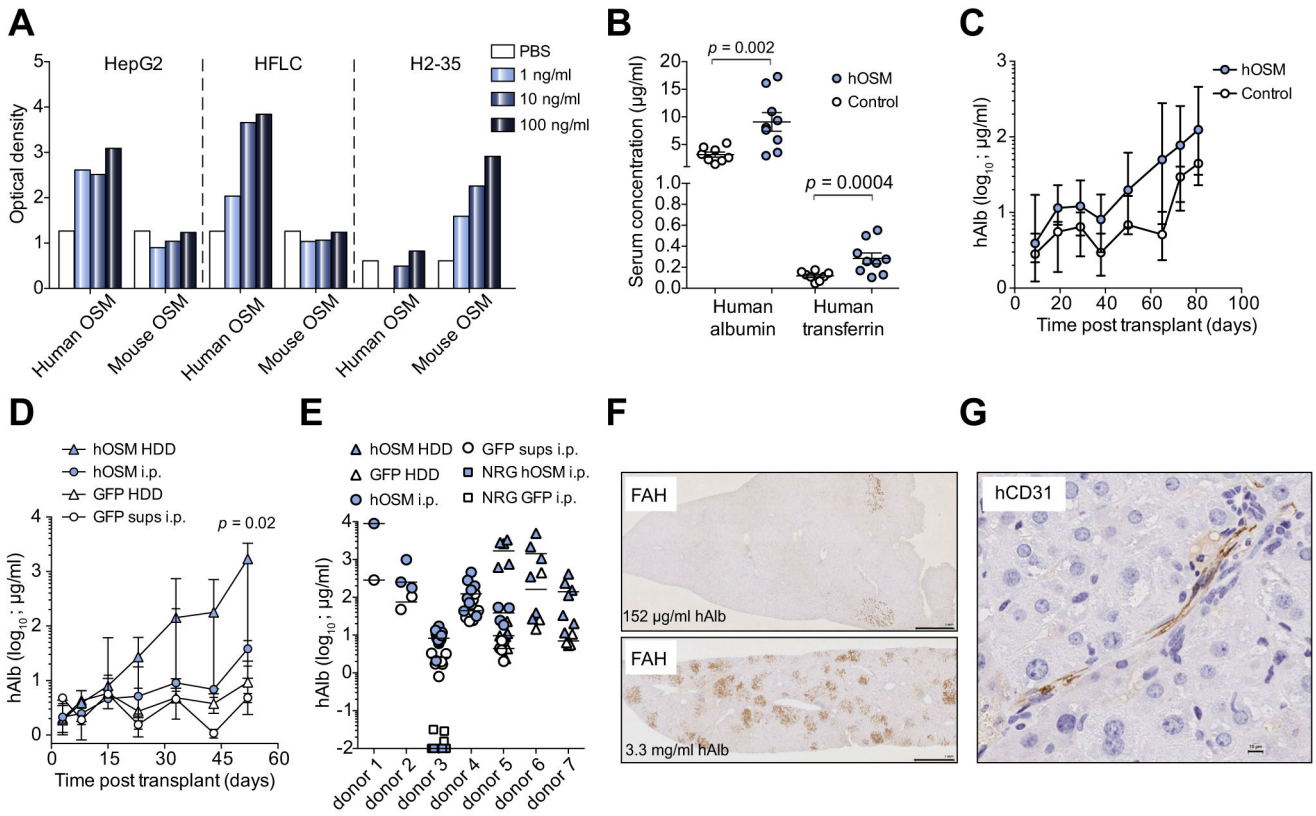

Fig. 1. Human oncostatin-M enhances human hepatoblast engraftment

(A) STAT3 phosphorylation was measured in human HepG2 hepatoma cells or primary human fetal liver cultures (HFLC) and mouse H2-35 cells by ELISA (B) hOSM was intraperitoneally (i.p.) injected daily into human hepatoblast transplanted FNRG mice for 3 weeks, and serum human albumin (hAlb) and transferrin (hTF) were measured on day 38 after transplantation and compared to PBS control-treated mice. (C) Median serum hAlb was measured in animals transplanted with human fetal hepatoblasts injected with either hOSM (filled circles, n = 9) or PBS control (open circles, n = 8). Error bars indicate range. (D) Comparison of hydrodynamic delivery (HDD) of an hOSM expressing plasmid before fetal hepatoblast transplantation (n = 5) and daily i.p. injections of hOSM (n = 6) (filled symbols). The control was a GFP plasmid (n = 6) or daily GFP supernatants (sups) i.p. injections (n = 6) (open symbols). Median and range hAlb serum levels are shown and *p* value compares hOSM HDD to hOSM i.p. (E) Determination of maximum serum hAlb levels of fetal hepatoblast transplanted animals from 7 donors, treated with hOSM injections or HDD (filled symbols). Control (PBS or GFP)-treated animals are shown in open symbols. Fetal hepatoblast transplanted NRG mice that do not suffer from mouse liver injury are shown in squares. (F) Detection of human hepatocytes by histochemical staining for fumaryl acetoacetate hydrolase (FAH) on FRG livers that were transplanted with human hepatoblasts (scale bar is 1 mm). (G) Human CD31 staining for endothelial cells in the liver of a mouse engrafted with human fetal hepatoblast (scale bar is 10 µm). Statistics: Mann-Whitney *U* test.

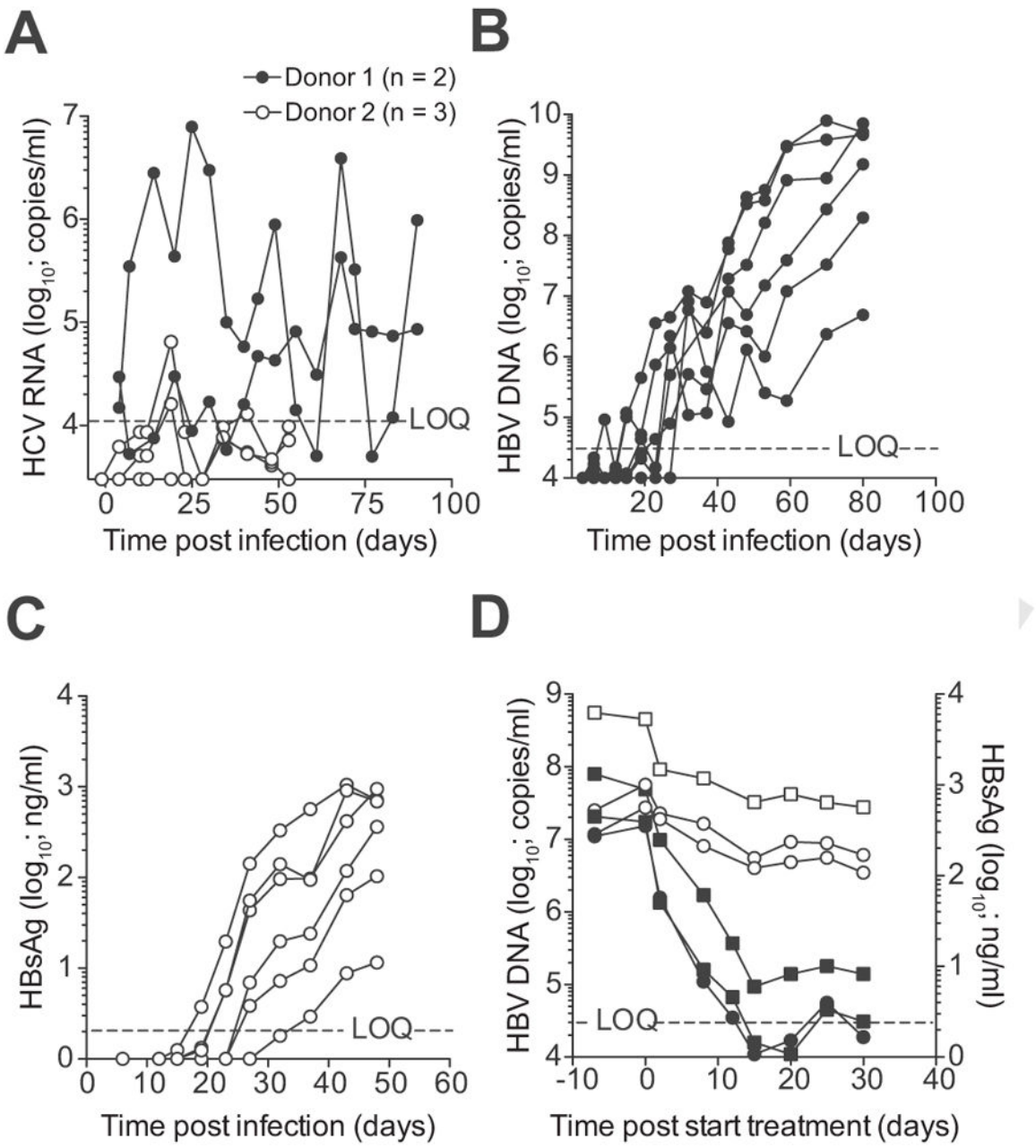

Fig. 2. Highly engrafted FRG mice support HBV and HCV infection

(A) FRG mice highly engrafted with human hepatoblasts from two donors were challenged with HCV and viremia was measured by qRT-PCR. (B) FRG mice with moderate to high liver engraftment were infected with plasma from an eAg negative HBV viremic patient. HBV viremia was quantified by qPCR. (C) HBsAg levels were quantified by chemiluminescence immunoassay in serum of FRG mice whose viremia is depicted in figure b. (D) Three mice stably viremic with eAg negative HBV were treated with daily i.p. injections (circles) or oral gavage (squares) of entecavir. HBV viremia (closed symbols) was determined by qPCR and HBsAg levels (open symbols) by CLIA. LOQ = limit of quantification for HBV DNA.

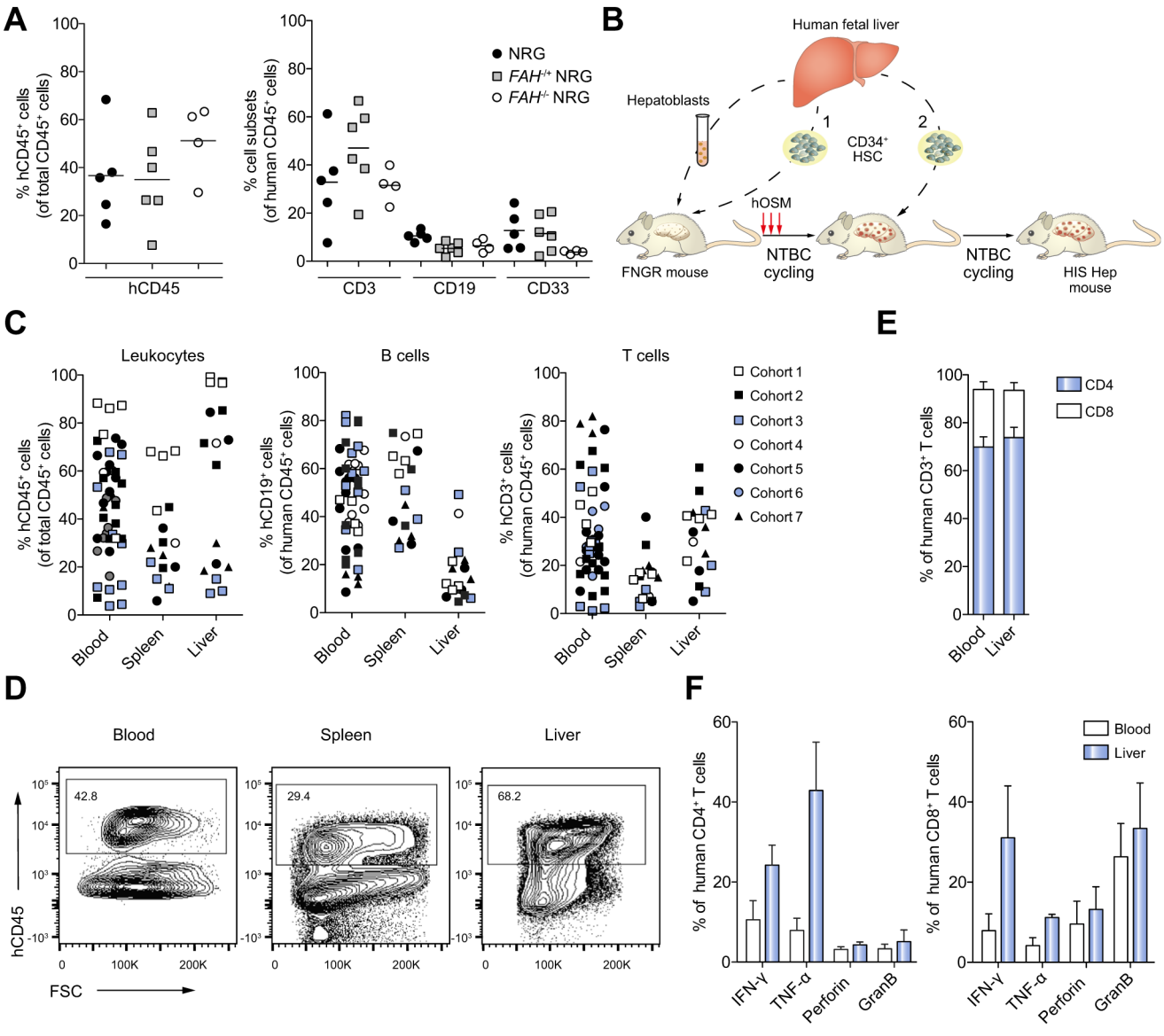

Fig. 3. Dual reconstitution with syngeneic human liver and immune cells

(A) Newborn NRG, *FAH*$^{-/+}$ NRG and *FAH*$^{-/-}$ NRG littermates were transplanted with CD34^{+} HSC from the same human donor. 12 weeks post transplantation human immune cell chimerism was analyzed. The left graph shows overall human CD45^{+} leukocyte reconstitution, the right graph shows CD3^{+} T cell, CD19^{+} B cell and CD33^{+} myeloid development in the blood. (B) Schematic showing the strategies used to generate FRNG mice with syngeneic human liver and immune cells (HIS-Hep mice) by either concurrent (1) or sequential (2) transplantation of hepatoblasts and CD34+ HSC. (C) Human CD45+ leukocyte, CD19^{+} B cell, and CD3+ T cell reconstitution in HIS-Hep mice. (D) FACS plots showing hCD45^{+} leukocytes in blood, spleen and liver of HIS-Hep mice. Plots are gated on total leukocytes. (e) Distribution of human CD4^{+} and CD8^{+} T cells in blood and liver of HIS-Hep mice (n = 7). (f) T cells were isolated from blood and liver (n = 7) and stimulated for 5 h with PMA/Ionomycin followed by intracellular cytokine staining. Graphs show

frequencies of IFN-γ, TNF-α, perforin and granzyme B producing $CD4^+$ (left) and $CD8^+$ (right) T cells.

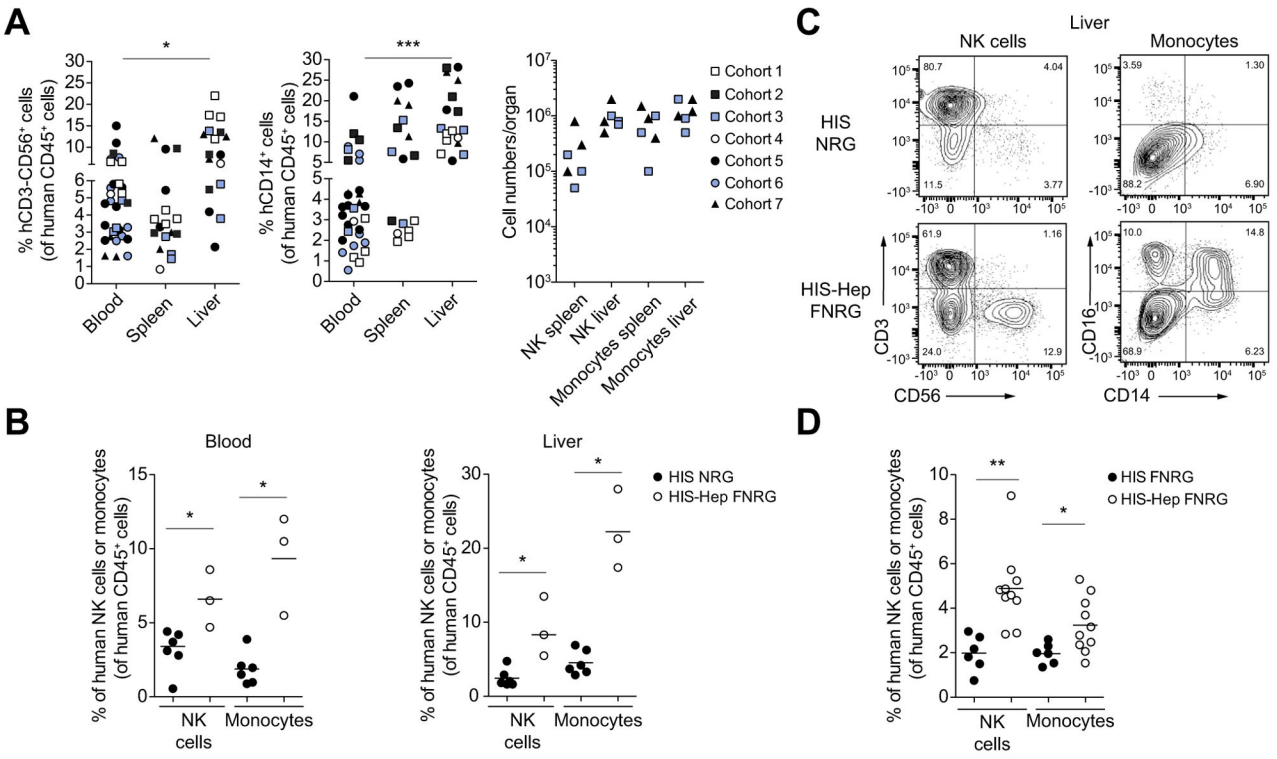

Fig. 4. Development of human monocytes and NK cells in HIS-Hep mice

(A) Human $CD56^{+}CD3^{-}$ NK cell, $CD14^{+}$ monocyte reconstitution and total splenic and intrahepatic monocyte and NK cell numbers in HIS-Hep mice at week 12-post HSC transplantation. (B) A cohort of HIS-NRG mice was generated in parallel with cohort 2 of HIS-Hep-FNRG mice using the same human $CD34^{+}$ HSC donor. Adult age-matched NRG and FNRG mice were compared in this experiment. Graphs show frequencies of human monocytes and NK cells in blood and liver. (C) FACS plots showing intrahepatic $CD56^{+}$ $CD3^{-}$ NK cells and $CD14^{+}/CD16^{+}$ monocytes in HIS-NRG and HIS-Hep-FNRG mice. Plots are gated on $hCD45^{+}$ leukocytes. (D) A cohort of HIS-FNRG mice was generated in parallel with cohort 3 of HIS-Hep FNRG mice using the same human $CD34^{+}$ HSC donor and the same NTBC cycling protocol to induce murine liver damage. Human NK cell and monocyte frequencies in the peripheral blood 8 weeks post HSC transplantation are shown. Statistics: Mann-Whitney *U* test: $^{*}p \leq 0.05$, $^{**}p \leq 0.005$, $^{***}p \leq 0.0005$.

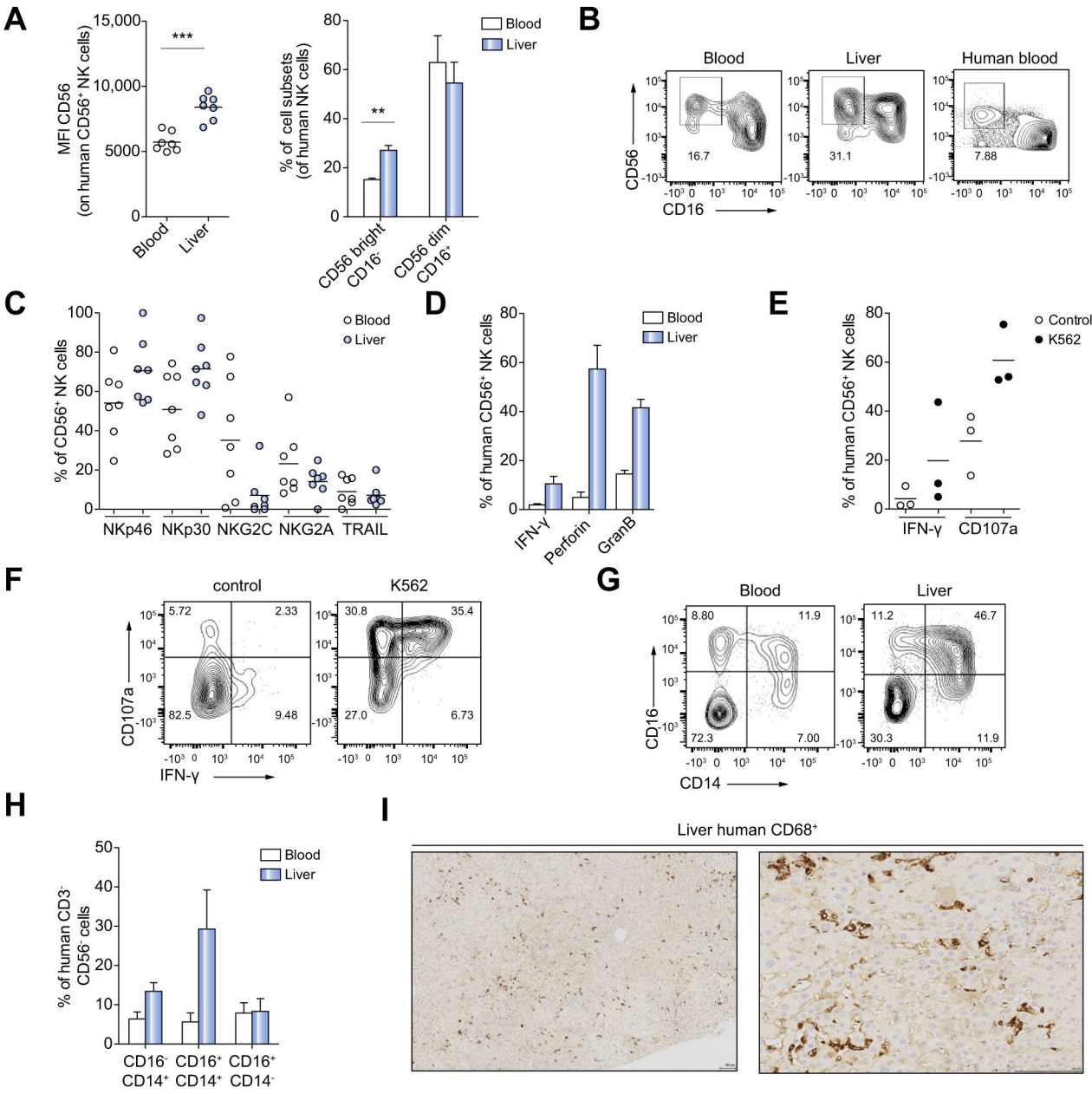

Fig. 5. Monocytes and NK cells of HIS-Hep mice resemble human counterparts in phenotype, function and tissue distribution

(A) NK cells of HIS-Hep mice were analyzed for CD56 and CD16 expression. CD56 mean fluorescence intensity (MFI) and frequencies of $CD56^{bright}CD16^{-}$ and $CD56^{dim}CD16^{+}$ subsets in blood and liver (n = 7). (B) FACS plots showing CD56 and CD16 expression levels of NK cells from HIS-Hep blood and liver and human peripheral blood. Plots are gated on $hCD45^{+}$ $CD3^{-}$ $CD56^{+}$ cells. (C) Surface expression of Nkp46, Nkp30, NKG2C, NKG2A and Trail on human NK cells in blood and liver of HIS-Hep mice (n = 7) (D) Blood and liver-derived NK cells of HISHep mice were stimulated for 5 h with PMA/Ionomycin followed by intracellular staining for IFN-γ, perforin and granzyme B (n = 4). (E) Liver-derived NK cells were cultured for 5 h with or without the human NK target cell line K562

in the presence of anti human CD107a antibody followed by intracellular IFN- γ staining (n = 3) (F) FACS plots showing IFN-γ production and degranulation (CD107a) of NK cells in presence or absence of K562 cells. Plots are gated on $hCD45^+$ $CD3^-$ $CD56^+$ cells. (G) FACS plots showing CD14 and CD16 expression on human peripheral and intrahepatic leukocytes. Cells are gated on $hCD45^+$ $CD3^-$ $CD56^-$ cells. (H) Frequencies of $CD16^-$ $CD14^+$, $CD16^+$ $CD14^+$ and $CD16^+$ $CD14^-$ monocytes within the $CD3^-$ $CD56^-$ cell population in blood and liver of HIS-Hep mice (n = 7) (I) Immunohistological staining of human $CD68^+$ monocytes in the liver of HIS-Hep mice. Scale bars are 100 μm in both panels. Statistics: Mann-Whitney *U* test: $^{*}p \leq 0.05$, $^{**}p \leq 0.005$, $^{***}p \leq 0.0005$.

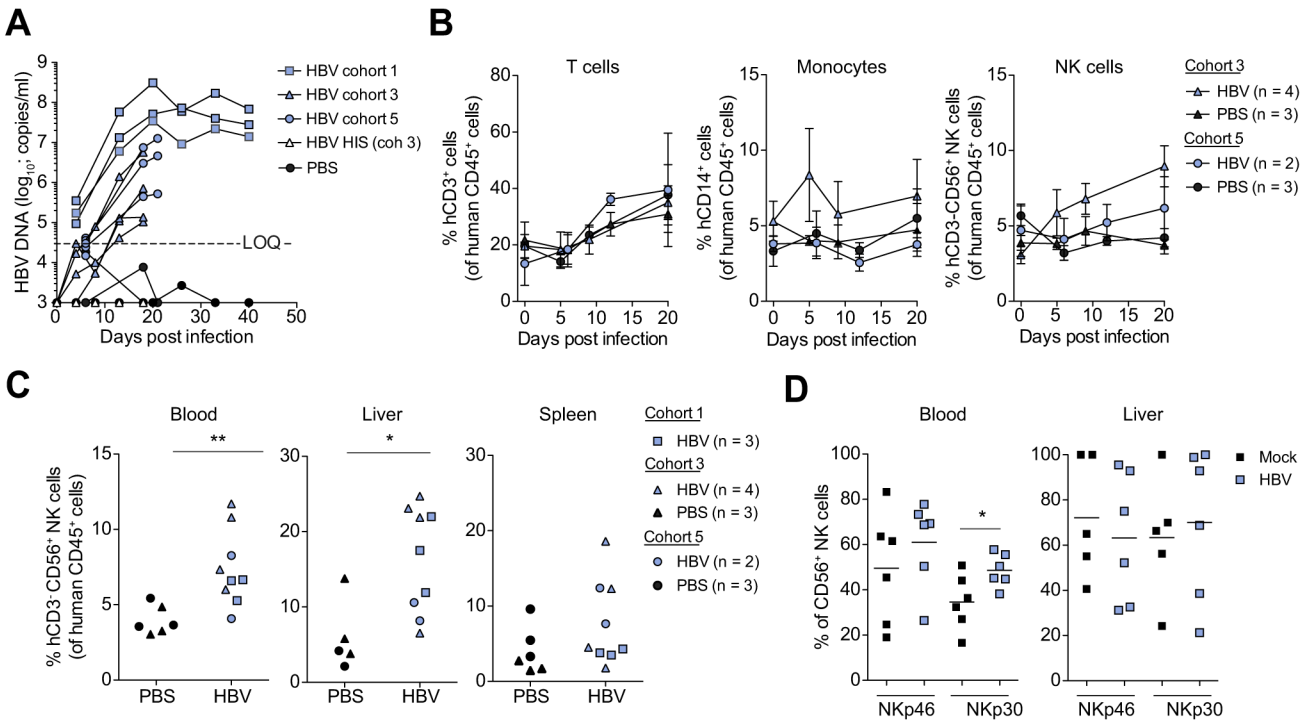

Fig. 6. Increased frequency of human NK cells during early HBV infection in HIS-Hep mice

(A) HIS-Hep mice were intravenously infected with 9.8×10^8 (cohort 1), 2.6×10^7 (cohort 3) and 3.5×10^6 (cohort 5) HBV genomes. HBV viral load was determined at multiple time points between day 0 and 40 post infection. (B) At day 0, 5, 9 and 20 post infection the peripheral blood of HIS-Hep mice from cohort 3 and 5 was analyzed for differences in $CD3^+$ T cell, $CD14^+$ monocyte and $CD56^+$ NK cell frequencies by flow cytometry. (C) At day 20 or 40 post HBV infection mice were sacrificed and NK cell frequencies in blood, spleen and liver were determined. (D) Expression levels of Nkp46 and Nkp30 on blood and liver derived NK cells of mice from cohort 3 and 5. Statistics: Mann-Whitney *U* test: $^{*}p \leq 0.05$, $^{**}p \leq 0.005$.